Article

The Binding Energy and Bonding in Dialane

Daniel J. Goebbert, Heriberto Hernandez, Joseph S. Francisco, and Paul G. Wenthold

J. Am. Chem. Soc., **2005**, 127 (33), 11684-11689• DOI: 10.1021/ja0424070 • Publication Date (Web): 27 July 2005

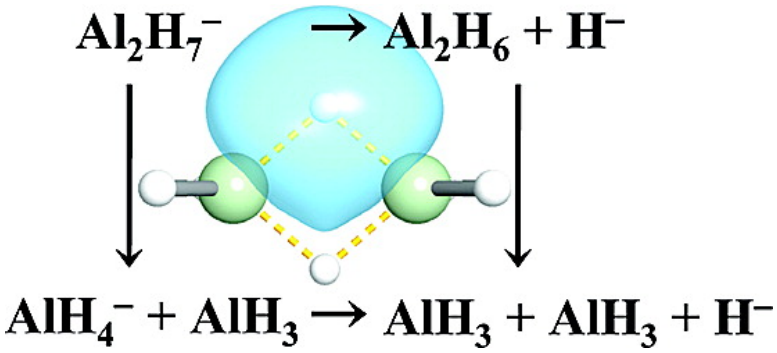

More About This Article

Additional resources and features associated with this article are available within the HTML version:

- Supporting Information
- Links to the 3 articles that cite this article, as of the time of this article download
- Access to high resolution figures
- Links to articles and content related to this article
- Copyright permission to reproduce figures and/or text from this article

View the Full Text HTML

J|A|C|S
ARTICLES
Published on Web 07/27/2005

The Binding Energy and Bonding in Dialane

Daniel J. Goebbert, Heriberto Hernandez, Joseph S. Francisco,* and Paul G. Wenthold*

Contribution from the Department of Chemistry, Purdue University, 560 Oval Drive, West Lafayette, Indiana 47907-2084

Received December 17, 2004; E-mail: pgw@purdue.edu

Abstract: The binding energy of dialane, Al_2H_6, has been measured using mass spectrometric techniques to be 33 ± 5 kcal/mol. This represents the first measurement of the thermochemical properties of dialane, which has only recently been observed in low-temperature matricies. High-level quantum mechanical calculations give a binding energy in agreement with the measured value. Experimental and quantum mechanical calculations show that dialane is chemically similar to diborane, B_2H_6, even though the bonding for these two systems shows significant differences.

In this report we describe a mass spectrometric measurement of the dissociation energy of dialane (Al_2H_6, Figure 1). Dialane is structurally similar to the well-known diborane, B_2H_6 (Figure 1), a classic example of an electron-deficient molecule with hydrogen μ-hydrido-bridge bonding.[1] However, whereas diborane can be readily synthesized[2] and is used extensively in the reduction of many organic compounds,[3] dialane is virtually unknown and is poorly characterized. Here we show that, while dialane has a binding energy and structure similar to those of diborane, the mode of bonding is very different.

Because of the importance of diborane, numerous physical studies have been carried out to establish its structure, stability, and properties. For example, the binding energy of diborane (eq 1) has been measured on many occasions, giving measured values between 36 and 59 kcal/mol.[4−8] Ab initio studies of the

$$B_2H_6 \rightarrow 2BH_3 \qquad (1)$$

binding energy of diborane have also been performed at various levels of theory and predict a binding energy between 38.8 and 47.2 kcal/mol,[9−11] within the range of the experimental values.

Aluminum is directly below boron on the periodic table and therefore should be expected to have many similar characteristics. However, unlike diborane, dialane has not been observed above ~6 K. In the solid state, AlH_3 forms a polymer with six-coordinate aluminum centers.[12,13] The only experimental investigations of the physical properties of dialane include matrix isolation infrared spectroscopy studies by Andrews et al.[14−16] and a photodetachment study reported by Rao and co-workers.[17] These studies confirm that dialane has a μ-hydrido-bridged structure, similar to that in diborane. However, nothing is known experimentally about the thermochemical properties of dialane or alane (AlH_3).

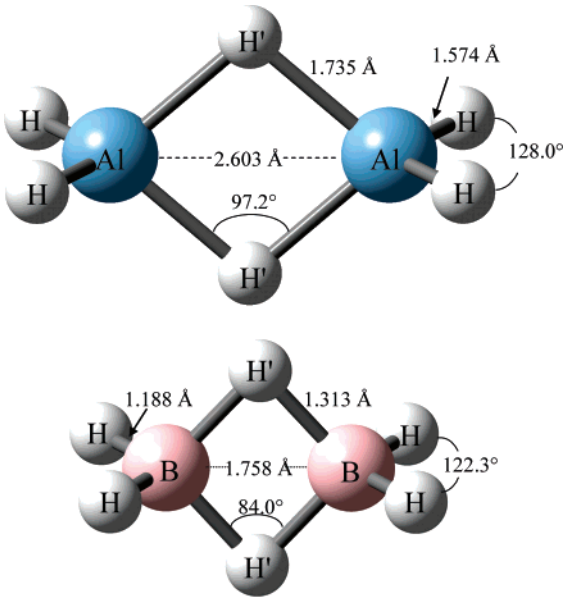

Figure 1. Optimized structures of Al_2H_6 and B_2H_6 at the CCSD(T) level of theory extrapolated to the complete basis set limit.

(1) Cotton, F. A.; Wilkinson, G.; Murillo, C. A.; Bochmann, M. *Advanced Inorganic Chemistry*, 6th ed.; Wiley: New York, 1999.
(2) Schlesinger, H. I.; Brown, H. C.; Abraham, B.; Davidson, N.; Finholt, A. E.; Lad, R. A.; Knight, J.; Schwartz, A. M. *J. Am. Chem. Soc.* **1953**, *75*, 191.
(3) Brown, H. C. *Boranes in Organic Chemistry*; Cornell University Press: Ithaca, NY, 1972.
(4) Fehlner, T. P.; Koski, W. S. *J. Am. Chem. Soc.* **1965**, *87*, 409.
(5) Fehlner, T. P.; Mappes, G. W. *J. Phys. Chem.* **1969**, *73*, 873.
(6) Burg, A. B.; Fu, Y. C. *J. Am. Chem. Soc.* **1966**, *88*, 1147.
(7) Gangule, P. S.; McGee, H. A., Jr. *J. Chem. Phys.* **1969**, *50*, 4658.
(8) Garabedian, M. E.; Benson, S. W. *J. Am. Chem. Soc.* **1964**, *86*, 176.
(9) Page, M.; Adams, G. F.; Binkley, J. S.; Melius, C. F. *J. Phys. Chem.* **1987**, *91*, 2675.
(10) Bock, C. W.; Trachtman, M.; Murphy, C.; Muschert, B.; Mains, G. J. *J. Phys. Chem.* **1991**, *95*, 2339.
(11) Barone, V.; Orlandini, L.; Adamo, C. *J. Phys. Chem.* **1994**, *98*, 13185.
(12) Turley, J. W.; Rinn, H. W. *Inorg. Chem.* **1969**, *8*, 18.
(13) Brown, F. M.; Matzek, N. E.; Reigler, P. F.; Rinn, H. W.; Roberts, C. B.; Schmidt, D. L.; Snover, J. A.; Terada, K. *J. Am. Chem. Soc.* **1976**, *98*, 2450.
(14) Andrews, L.; Wang, X. *Science* **2003**, *299*, 2049.
(15) Wang, X.; Andrews, L.; Tam, S.; DeRose, M. E.; Fajardo, M. E. *J. Am. Chem. Soc.* **2003**, *125*, 9218.
(16) Andrews, L.; Wang, X. *J. Phys. Chem. A* **2004**, *108*, 4202.
(17) Rao, B. K.; Jena, P.; Burkart, S.; Gantefor, G.; Seifert, G. *Phys. Rev. Lett.* **2001**, *86*, 692.

10.1021/ja0424070 CCC: $30.25

Table 1. Binding Energies of Dialane, $D_0(Al_2H_6)$[a]

method	energy (kcal/mol)	ref
theory		
MP4/6-31G**	31.5	19
MP2(FULL)/6-31G**	31.5	10
CCSD/DZP	30.8	20
B3LYP/TZ2Pf	33.3	12
CCSD(T)/aug-cc-PVDZ	29.6	this work
CCSD(T)/aug-cc-PVTZ	32.9	this work
CCSD(T)/aug-cc-PVQZ	33.5	this work
CBS limit	34.3	this work
experiment		
mass spectrometry	33 ± 5	this work

[a] 0 K binding energy (zero-point energy included), D_0.

Scheme 1

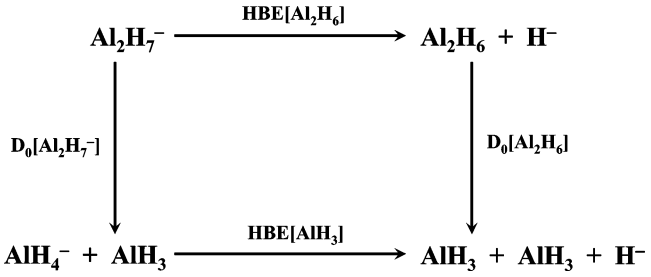

Extensive theoretical calculations have been carried out to predict the physical properties of Group 13 hydrides.[11,18−20] The binding energies of the M_2H_6 molecules (M = B, Al, and Ga) are predicted to decrease down the period. For example, at the B3LYP level of theory using a triple-ζ basis set, the binding energies are 39.9, 33.3, and 23.1 kcal/mol for diborane, dialane, and digallane, respectively.[11] Thus, although dialane readily polymerizes, it is predicted to be a stable species.[14,21] A summary of the calculated binding energies of dialane is given in Table 1.

We have determined the energy for dissociation of Al_2H_6 into two molecules of AlH_3 by using mass spectrometry. The dissociation energy of dialane, $D_0(Al_2H_6)$, is related to the hydride binding energies (HBEs) of AlH_3 and Al_2H_6, which are the 0 K energies for the reaction type in eq 2, and the dissociation energy of $Al_2H_7^-$, eq 3, as outlined in Scheme 1.

$$MH^- \rightarrow M + H^- \quad (2)$$

$$Al_2H_7^- \rightarrow AlH_4^- + AlH_3 \quad (3)$$

Our studies find that the measured dissociation energy of Al_2H_6 is only slightly less than that in B_2H_6, in good agreement with theoretical predictions, and that the large difference in the reactivity of B_2H_6 and Al_2H_6 is not due to differences in the dimer stability. Natural bond order and resonance theory analyses indicate that the reactivity differences are likely due to differences in the polarity of the B−H and Al−H bonds.

Experimental Section

All measurements were made using a flowing-afterglow triple-quadrupole mass spectrometer that has been described previously.[22] Aluminum hydride ions were produced by electron ionization (EI) of dimethylethylamine−alane (DMEAA, 0.5 M solution in toluene) in a high-pressure flow tube containing He buffer gas (P(He) = 0.4 Torr, flow(He) = 200 STP cm^3/s). Ions generated in the flow tube are cooled to 298 ± 2 K by ca. 10^5 collisions with the He gas. Negative ions are extracted through a 1-mm orifice by application of a small positive voltage (1 V) and focused into a low-pressure triple-quadrupole mass analyzer, where the ions can be mass analyzed in the first or third quadrupoles, Q1 and Q3, and can be subjected to collision-induced dissociation (CID) or reactions with neutral gases in the rf-only collision cell, Q2. Product ions are detected by an electron multiplier operating in pulse-counting mode. Absolute cross sections from CID experiments were calculated using the expression $\sigma_p = I_p/(INl)$, where I_p and I are the intensities of the product and reactant ion respectively, N is the number density of the neutral gas, and l is the path length for the reaction. The effective path length was obtained from calibration experiments using the reaction $Ar^+ + D_2 \rightarrow ArD^+ + D$, which has an established reaction cross section.[23] The ion translational energy in Q2 is varied by changing the Q2 rod offset voltage, which is the laboratory frame energy, E_{lab}, and the energy origin is obtained by retarding potential analysis. Reaction energies are converted to the center-of-mass frame (E_{CM}) by using $E_{CM} = E_{lab}(m/(m + M))$, where m and M are the masses of the neutral and the ion, respectively. The reaction cross sections are also measured at multiple pressures of the neutral reactant gas, and ion intensities are linearly extrapolated to zero pressure prior to analysis of the data.

Data Analysis. Product cross sections were measured as a function of Q2 collision energy to yield energy-resolved mass spectra (ERMS), which are modeled (eq 4) using standard procedures described elsewhere.[24−29] In this model, $\sigma(E)$ is the reaction cross section at the

$$\sigma(E) = \sigma_0 \sum_i g_i P_i (E + E_i - E_0)^n / E \quad (4)$$

collision energy E, and σ_0 is an energy-independent scaling factor. The sum is over the vibrational energy distributions of the ionic and neutral reactants having a population g_i and energy E_i, whereas n is an adjustable parameter that reflects the energy deposition during the collision event.[30] The parameter P_i in eq 4 is the probability, calculated by using RRKM theory,[27] that the reactant ion with total internal energy $E + E_i$ will give the product on the instrument time scale. This model is used to fit the experimental data by varying the parameters σ_0, E_0, and n to minimize the deviation from the ERMS cross sections in the steeply rising portion of the curve directly above the energy onset. The quantity E_0, obtained from the fitting, is the 0 K reaction energy, ΔE_0, and can be converted to 298 K enthalpy (ΔH_{298}), if desired, by using the integrated heat capacities of reactants and products. The internal energy distributions required for the modeling and the heat capacities for the reactants and products were generally obtained by using vibrational frequencies and rotational constants calculated at the CCSD-(T)/aug-cc-pVTZ level of theory. The analysis was performed using the CRUNCH program written by Armentrout and co-workers.[25,26,29,31]

(18) Lammertsma, K.; Leszczynski, J. *J. Phys. Chem.* **1990**, *94*, 2806.
(19) Shen, M.; Schaefer, H. F., III. *J. Chem. Phys.* **1992**, *96*, 2868.
(20) Liang, C.; Davy, R. D.; Schaefer, H. F., III. *Chem. Phys. Lett.* **1989**, *159*, 393.
(21) Downs, A. J.; Greene, T. M.; Johnsen, E.; Brian, P. T.; Morrison, C. A.; Parsons, S.; Pulham, C. R.; Rankin, D. W. H.; Aarset, K.; Mills, I. M.; Page, E. M.; Rice, D. A. *Inorg. Chem.* **2001**, *40*, 3484.
(22) Marinelli, P. J.; Paulino, J. A.; Sunderlin, L. S.; Wenthold, P. G.; Poutsma, J. C.; Squires, R. R. *Int. J. Mass Spectrom. Ion Processes* **1994**, *130*, 89.
(23) Ervin, K. M.; Armentrout, P. B. *J. Chem. Phys.* **1985**, *83*, 166.
(24) Chesnavich, W. J.; Bowers, M. T. *J. Phys. Chem.* **1979**, *83*, 900.
(25) Sunderlin, L. S.; Armentrout, P. B. *Int. J. Mass Spectrom. Ion Processes* **1989**, *94*, 149.
(26) Schultz, R. H.; Crellin, K. C.; Armentrout, P. B. *J. Am. Chem. Soc.* **1991**, *113*, 8590.
(27) Rodgers, M. T.; Ervin, K. M.; Armentrout, P. B. *J. Chem. Phys.* **1997**, *106*, 4499.
(28) Ervin, K. M. *Chem. Rev.* **2001**, *101*, 391.
(29) Armentrout, P. B. *J. Am. Soc. Mass Spectrom.* **2001**, *13*, 419.
(30) Muntean, F.; Armentrout, P. B. *J. Chem. Phys.* **2001**, *115*, 1213.
(31) Armentrout, P. B.; Ervin, K. M. CRUNCH 5, 1995−2005.

Uncertainties in E_0 values include the standard deviations obtained from replicate measurements, a 0.15 eV (laboratory frame) contribution due to uncertainty in the absolute energy scale, and a contribution due to uncertainty in the transition state, estimated as the change in the threshold energy that results from changing the activation entropy by ±2 cal/mol·K. For the systems examined in this work, the choice of transition state does not have a large effect on the modeled dissociation energy, and the uncertainty contribution is ca. 0.01 eV.

Materials. A 0.5 M solution of DMEAA in toluene was obtained from Sigma-Aldrich. All other reagents were also obtained from commercial suppliers and used as received.

Results and Discussion

Thermochemical Measurements. The HBEs of AlH_3 and Al_2H_6 were obtained by measuring the energy for hydride transfer between AlH_4^- and $Al_2H_7^-$, respectively, and CO_2, as shown in eq 5.

$$AlH_4^- + CO_2 \rightarrow AlH_3 + HCO_2^- \qquad \Delta E_{rxn} = \Delta E_0(AlH_4^-) \quad (5a)$$

$$Al_2H_7^- + CO_2 \rightarrow Al_2H_6 + HCO_2^- \qquad \Delta E_{rxn} = \Delta E_0(Al_2H_7^-) \quad (5b)$$

The hydride affinities (HA, the 298 K enthalpy required for eq 2) of AlH_3 and Al_2H_6 can be obtained by using eq 6, which combines the enthalpies of the reactions in eq 5, derived from the reaction energies by using the integrated heat capacities of the reactants and products, and the HA of CO_2 (52 ± 2 kcal/mol).[3232] This approach for measuring the hydride affinity is analogous to that used previously by Workman and Squires to determine the HA of borane.[3333]

$$HA(AlH_3) = HA(CO_2) + \Delta H_{298}(AlH_4^-) \quad (6a)$$

$$HA(Al_2H_6) = HA(CO_2) + \Delta H_{298}(Al_2H_7^-) \quad (6b)$$

Electron ionization of a 0.5 M solution of DMEAA in toluene gives four major peaks at *m*/*z* 31, 61, 88, and 134, which are assigned to AlH_4^-, $Al_2H_7^-$, $[DMEAA - CH_3]^-$, and $[DMEAA + AlH_4]^-$, respectively. Under certain conditions it is possible to observe small amounts of *m*/*z* 91 and 121, which correspond to the higher order alane polymers $Al_3H_{10}^-$ and $Al_4H_{13}^-$. The ions *m*/*z* 31 and 61 displayed very little reactivity with any reagents, including potential hydride acceptors such as CO_2, SO_2, $(CH_3)_2CO$, CH_3CHO, and CH_3CN. Although AlH_4^- in solution is used in the reductions of aldehydes, ketones, and many other functional groups,[34] the lack of reactivity of AlH_4^- in the gas phase is not surprising given the large hydride binding energy (vide infra). Similar results have been observed with gaseous BH_4^-, also unreactive with these species.[33]

The energy-resolved reactivity of the ion with *m*/*z* 31 confirms that it is indeed AlH_4^- and not the isobar methoxide, CH_3O^-. The relative cross sections for hydride transfer between *m*/*z* 31 generated from DMEAA and authentically prepared CH_3O^- with CO_2 have been measured (Figure S1, Supporting Information), and significant differences are observed for the HCO_2^- products obtained from the two reactants. The cross section for formation of HCO_2^- from CH_3O^- has a maximum near 0 eV, and drops precipitously at higher energies, consistent with what is expected for an exothermic reaction. This behavior agrees with that expected because the HA of CO_2 is greater than that of H_2CO (41 ± 1 kcal/mol).[32] The appearance curve for HCO_2^- from DMEAA generated *m*/*z* 31 has a distinctly different shape (Figure 2), with an onset near 1 eV, indicating an endothermic hydride transfer. CID experiments with larger ions formed upon EI confirm that they contain AlH_4^-, as an ion with *m*/*z* 31 is the major product in all cases. In addition, the *m*/*z* 61 ion undergoes endothermic hydride transfer with CO_2, consistent with what is expected for $Al_2H_7^-$.

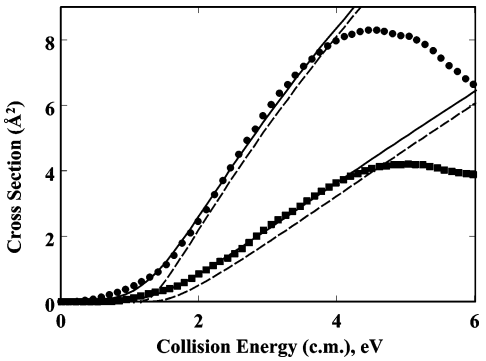

Figure 2. Energy-resolved mass spectra for formation of HCO_2^- from the reactions of AlH_4^- (●) and $Al_2H_7^-$ (■) with CO_2. The dashed lines show the fit of eq 5 for ions with no internal energy, while the solid lines include internal energy distributions and are convoluted with the kinetic energy distribution of the reactants.

The cross sections for formation of HCO_2^- from hydride transfer of AlH_4^- and $Al_2H_7^-$ to CO_2 are shown in Figure 2, along with the fits to the data. Modeling the cross sections using the procedures described above yields hydride transfer ΔE_0 values of 23 ± 3 and 27 ± 2 kcal/mol using AlH_4^- and $Al_2H_7^-$, respectively. However, the ΔE_0 value obtained for the reaction of $Al_2H_7^-$ with CO_2 was obtained without considering the effect the presence of the available CID channel has on the measured onset for reaction. Because the second channel can potentially lead to a competitive shift in the data, the measured reaction energy is technically an upper limit.[27]

To determine the effect of the competitive shift on the measured reaction energy, we have modeled the processes by using RRKM theory to determine the branching ratios for the two channels. If the transition-state structures for the reactions are known, or can be reasonably approximated, then the probabilities of forming each product can be determined from the corresponding partition functions. The transition-state structures are not known for the present system, but, fortunately, if one transition state for a multichannel process can be assigned, then the properties of the transition states for the remaining channels can be determined empirically. In this case, the transition state for CID is assumed to be the orbiting transition state, in the phase-space limit, as described previously by Rodgers and Armentrout.[27] Given that assumption, the properties of the transition state for the hydride transfer, reflected in the activation entropy, can be determined by systematically adjusting the set of ro-vibrational constants in order to obtain the best agreement between the calculated model and the data. We have recently used this type of approach to model the cross sections

(32) Bartmess, J. E. Negative Ion Energetics Data. In *NIST Chemistry WebBook*; Mallard, W. G., Linstrom, P. J., Eds.; NIST Standard Reference Database No. 69; National Institute of Standards and Technology: Gaithersburg, MD, March 2003.
(33) Workman, D. B.; Squires, R. R. *Inorg. Chem.* **1988**, *27*, 1846.
(34) Smith, M. B.; March, J. *Advanced Organic Chemistry*, 5th ed.; John Wiley & Sons: New York, 2001.

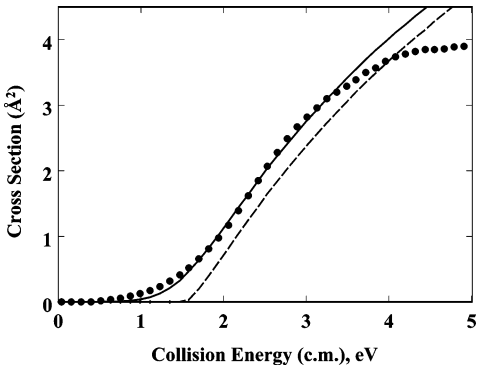

Figure 3. Energy-resolved mass spectra for formation of AlH_4^- from CID of $Al_2H_7^-$ with argon target. The dashed line shows the fit of eq 5 for ions with no internal energy, while the solid line includes the internal energy distribution and kinetic energy distributions of the reactants.

for the multichannel decomposition of fluorosiliconate ions[35] and protonated butanedione.[36] It is important to note that, with the assumption of the orbiting transition state for the CID process, the rest of the system is completely determined, and the activation entropy for the competing process can be optimized along with the other adjustable parameters (ΔE_0 values, n, σ_0).

To model the competitive reactions, we initially fit the data using the same transition state for both reaction channels, the orbiting transition state for CID. The vibrational frequencies for the transition state for the hydride-transfer channel were then scaled, changing the activation entropy, and the data were fit again over the same energy range (1−4 eV, which includes the steeply rising portions of both appearance curves). The fitting results obtained with different transition-state parameters for a representative data set, along with the resulting χ^2 values, are shown in Table S1 (Supporting Information). In general, the optimal fit was obtained when the transition-state parameters for hydride transfer were essentially the same as those for CID. Although the activation entropies for the two reactions are similar, this does not mean that the two reactions necessarily have the same transition state; it only indicates that the partition functions for the two transition states are similar. The hydride transfer ΔE_0 value for $Al_2H_7^-$ is 0.07 eV (2 kcal/mol) lower when the competitive shift is taken into account, leading to a reaction energy of 25 ± 3 kcal/mol, where the uncertainty includes a 2 kcal/mol component to account for uncertainty in the competitive shift treatment in addition to those components described in the Experimental Section.

Converting the hydride transfer ΔE_0 values to 298 K enthalpies and combining them with $HA(CO_2)$, we obtain $HA(AlH_3) = 75 \pm 4$ kcal/mol and $HA(Al_2H_6) = 77 \pm 4$ kcal/mol. The measured hydride affinities compare well with theoretical predictions of $HA(AlH_3) = 73.7$ kcal/mol and $HA(Al_2H_6) = 78.5$ kcal/mol obtained at the B3LYP/6-311++G(3df,3pd) level of theory, and are similar to the hydride affinity of borane, $HA(BH_3) = 74.2 \pm 2.8$ kcal/mol.[33]

The dissociation energy of $Al_2H_7^-$ was obtained by modeling the cross sections for collision-induced dissociation with Ar target (Figure 3). Although it is possible to determine the dissociation energy from the CO_2 CID cross sections, argon is a better target because CID is the only process that occurs, and it is not necessary to account for competitive shifts, as described above. Analysis of these data using eq 5 gives a dissociation enthalpy, D_0, of 35 ± 2 kcal/mol. The value of D_0 obtained when using CO_2 as the collision gas, with the modeling described above, is experimentally indistinguishable from that obtained when using the inert target. The quantity $D_0(Al_2H_7^-)$ can be combined with the HBEs of AlH_3 and Al_2H_6, according to Scheme 1, to obtain the dimerization energy of dialane. However, the calculation can be simplified because the absolute values of $HBE(AlH_3)$ and $HBE(Al_2H_6)$ both depend on the value for CO_2, and therefore, as shown in eq 7, the HBE of CO_2 is not required to determine the bond dissociation energy. By using the measured energies for $\Delta E_0(AlH_4^-)$, $\Delta E_0(Al_2H_7^-)$, and $D_0(Al_2H_7^-)$, the 0 K dissociation energy of dialane into two alane molecules is calculated to be 33 ± 5 kcal/mol.

$$\begin{aligned} D_0(Al_2H_6) &= HBE(AlH_3) + D_0(Al_2H_7^-) - HBE(Al_2H_6) \\ &= \Delta E_0(AlH_4^-) + HBE(CO_2) + D_0(Al_2H_7^-) - \\ &\qquad \Delta E_0(Al_2H_7^-) - HBE(CO_2) \\ &= \Delta E_0(AlH_4^-) + D_0(Al_2H_7^-) - \\ &\qquad \Delta E_0(Al_2H_7^-) \quad (7) \end{aligned}$$

Theoretical Studies of Dialane Thermochemistry and Bonding. State-of-the-art quantum mechanical calculations have also been performed on dialane to investigate its bonding.[37] For comparison, calculations were also carried out on diborane. The binding energies of dialane and diborane were calculated using coupled-cluster theory, CCSD(T). Structures, energies, and frequencies were calculated using the aug-cc-pVDZ, aug-cc-pVTZ, and aug-cc-pVQZ basis sets, and the results were extrapolated to the complete basis set (CBS) limit (Figure 1). To extrapolate to the CBS limit for the CCSD(T) total energies, a three-parameter mixed exponential Gaussian function is used, shown in eq 8, where n = 2(DZ), 3(TZ), and 4(QZ), as first proposed by Peterson et al.[38] At this level of theory, the

$$E(n) = E_\infty + A \exp[-(n-1)] + B \exp[-(n-1)^2] \quad (8)$$

difference in zero-point energy (ZPE)-corrected electronic energies between two alane molecules and dialane is 34.3 kcal/mol, 3 kcal/mol smaller than that calculated for diborane (37.5 kcal/mol). The calculated value for the dissociation energy of dialane agrees with the experimentally measured value of 33 ± 5 kcal/mol. It is interesting to note that the dissociation energy for diborane calculated directly from the computed electronic energies is ca. 7 kcal/mol larger than that for dialane, whereas the dissociation energies corrected for ZPE are closer, giving the impression of similar bonding in diborane and dialane. However, this observation is misleading because there are significant differences in the ZPE components of the BDE because of the mass difference between Al relative to B and the large force constants in diborane relative to dialane. These corrections give the impression that the systems are more similar than they actually are. The large difference in zero-point energy

(35) Krouse, I. H.; Lardin, H. A.; Wenthold, P. G. *Int. J. Mass Spectrom.* **2003**, *227*, 303.
(36) Liu, X.; Gross, M. L.; Wenthold, P. G. *J. Phys. Chem. A* **2005**, *109*, 2183.
(37) Frisch, M. J.; et al. *Gaussian 03*, Revision B.05; Gaussian, Inc.: Pittsburgh, PA, 2003.
(38) Peterson, K. A.; Woon, D. E.; Dunning, T. H., Jr. *J. Chem. Phys.* **1994**, *100*, 7410.

Table 2. Atomic Charges and Bond Orders in Al_2H_6 and B_2H_6

	charges					bond orders		
species	Al	B	H′	H	coordinate	covalent contribution	ionic contribution	total
Al_2H_6	1.09		−0.40	−0.35	Al−H	0.62	0.35	0.97
					Al−H′	0.15	0.31	0.46
					Al−Al	0.00	0.04	0.04
B_2H_6		−0.09	0.10	0.00	B−H	0.97	0.0	0.97
					B−H′	0.23	0.21	0.44
					B−B	0.24	0.28	0.52

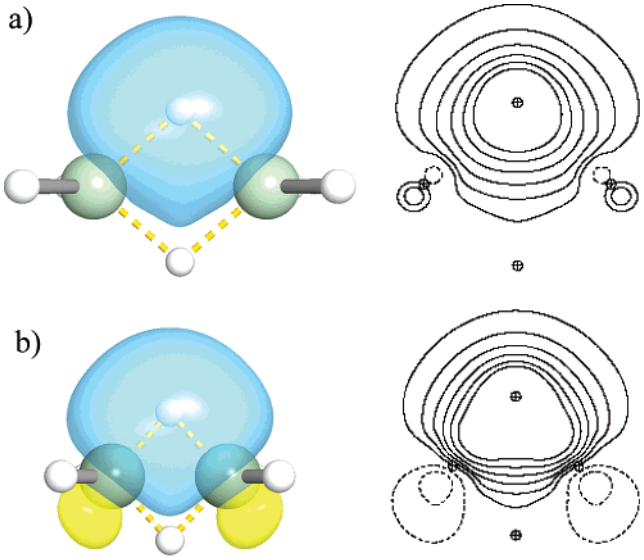

Figure 4. 3D views and contour plots of one of the two symmetrically equivalent orbitals comprising a τ bond in (a) Al_2H_6 and (b) B_2H_6 and the corresponding orbital hybridizations; $\tau_{Al-H-Al} = 0.38(sp^{6.6})_{Al} + 0.84(s)_H + 0.38(sp^{6.6})_{Al}$ and $\tau_{B-H-B} = 0.52(sp^{4.7})_B + 0.67(s)_H + 0.52(sp^{4.7})_B$, respectively.

correction for dialane and diborane is due to the large differences in the vibrational frequencies in Al_2H_6 and B_2H_6, resulting from the differences in the bonding of the two species, described below.

A detailed analysis of the bonding in dialane and diborane has been carried out by using the natural bond orbital (NBO) and natural resonance theory (NRT) methods.[39,40] The NBO approach, carried out using the MP2/aug-cc-pVTZ wave function, reveals that a three-center, two-elecron bond is formed in Al_2H_6 and B_2H_6. This type of bond is known as a tau bond (τ) and is found in hypovalent molecules.[41] Figure 4 shows 3D views and the contour plots of the τ bond in Al_2H_6 and B_2H_6. We find that the hybrid orbitals that constitute the τ bonds in dialane and diborane are different due to differences in mixing of s and p orbitals from Al and B. In addition, the s orbital on the hydrogen atom contributes more to the formation of the τ bond in dialane than it does for diborane. The hybridization of the τ bond in diborane shows that the boron orbital coefficients are 0.52 and the hydrogen orbital coefficient is 0.67, indicating that all three hybrid orbitals have similar contributions in the formation of the τ bond, and therefore the τ bond will show s and p character, as shown in Figure 4b. On the other hand, the coefficients in Al_2H_6 are 0.38 on the Al and 0.84 on the hydrogen. Therefore, despite there being greater p character in the aluminum-based orbitals, there is less p character in the τ bonding orbital, as can be seen in the contour plots in Figure 4a.

Another property that illustrates the difference in bonding between Al_2H_6 and B_2H_6 is the charge distribution. Table 2 shows the NBO charges for the two species. There is a large difference in the charges of the Al (1.09) and the bridge hydrogen (−0.40) in dialane compared to the difference in charge of boron (−0.09) and the bridge hydrogen (0.10) in diborane. These results indicate that the bonding character in dialane is more ionic than that in diborane. Pauling electronegativities of boron and hydrogen are 2.0 and 2.1, respectively, such that the bonds between them should be highly covalent. However, the electronegativity of aluminum is only 1.5, such that bonds between aluminum and hydrogen should be polar with the electrons drawn to the hydrogen, as in the ionic structure Al^+-H^-. The ionic character of the bonds in dialane and diborane is evident in the calculated bond orders between the atoms in the molecules, shown in Table 2.

The bond orders in Table 2 are divided in terms of their covalent and ionic contributions to the total bond order. The Al−H′ portion of the τ bond in Al_2H_6 (Al−H′ in Table 2) is 67% ionic and 33% covalent, whereas in B_2H_6 the B−H′ bond is about 50% covalent and 50% ionic. Similarly, the bonds to the nonbridging hydrogens in Al_2H_6 (Al−H) are 64% covalent and 36% ionic, whereas those in diborane are purely covalent. The differences in the ionic character of the bonds are consistent with the differences in the calculated charge distributions. Another significant difference in the bonding is in the interactions between the non-hydrogen atoms. In Al_2H_6 there is essentially no interaction between the aluminum atoms, in contrast to diborane, where the bond order between boron atoms is 0.5. The differences in charge distributions are also reflected in the quadrupole moments, where the XX, YY, and ZZ components of the quadrupole moment of dialane are calculated to be twice as large as those for diborane.

The bonding differences between diborane and dialane can be appreciated by comparing the resonance structures that constitute the wave functions, shown in Figure 5. The Pauling concept of the chemical bond using resonance structures provides a pictorial description of the bonding in molecular systems. This analysis is based on the HF wave functions calculated at the optimized coupled-cluster geometries. The NRT breakdown of the wave function in B_2H_6 is shown in the left half of Figure 5. The main resonance structures include those such as that shown in Figure 5a, which result from hydride transfer; Figure 5b, structures resembling two boranes; Figure

(39) Reed, A. E.; Weinhold, F. J. *J. Chem. Phys.* **1983**, *78*, 4066.
(40) Foster, J. P.; Weinhold, F. J. *J. Am. Chem. Soc.* **1980**, *102*, 7211.
(41) Weinhold, F. J.; Landis, C. R. *Valency and Bonding: A Natural Bond Orbital Donor−Acceptor Perspective*; Cambridge University Press: Cambridge, 2003.

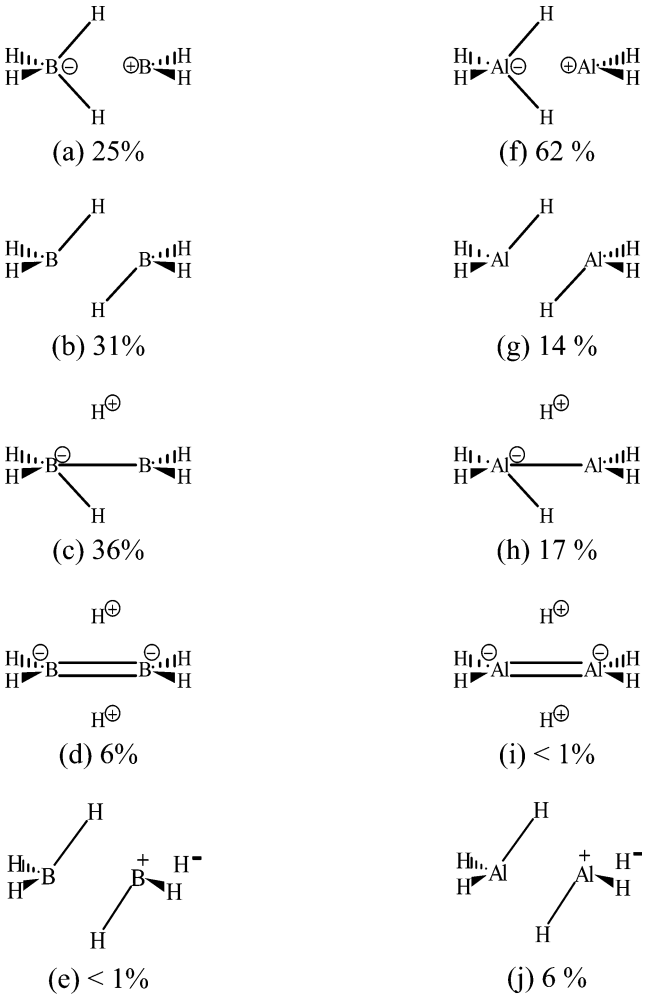

Figure 5. Main resonance structures for (a−e) B_2H_6 and (f−j) Al_2H_6.

5c, structures consisting of a proton and a boron-substituted borohydride; and Figure 5d, a structure with a double bond between the borons. The largest contribution is from the structures shown in Figure 5a−c, but all four structures contribute significantly to the wave function and account for 98% of the total. None of the other resonance structures contributes more than 1%. The resonance picture of diborane shown in Figure 5 is similar to that reported previously by Weinhold and Landis.[40] In contrast, Al_2H_6 has one main resonance structure, shown in Figure 5f, which results from hydride transfer and makes up 62% of the wave function. The most notable difference between dialane and diborane is that the other ionic structures, shown in Figure 5h,i, are much less important for dialane than for diborane. These resonance structures are less important for dialane because they require charge polarization opposite to that predicted by the electronegativity differences of the atoms. The significantly lower contributions from these structures in Al_2H_6 account for the lower bond order between the non-hydrogen atoms in that system. Structures like that shown in Figure 5j, which lead to polarization of the Al−H bonds, constitute about 6% of the wave function for dialane, but are not part of the diborane wave function.

Conclusion

Detailed electronic structure properties show very different bonding in diborane and dialane due to the large difference in the polarity of B−H and Al−H bonds. Ultimately, however, the differences in bonding produce only a small difference in the stability of the two molecules, as the measured energies for dissociation into borane or alane monomers are within 5 kcal/mol. The results indicate that thermodynamic instability of dialane is not the reason that it is not readily isolable like diborane. Similarly, gas-phase studies find similar thermochemical properties for borohydrides (BH_4^-, $B_2H_7^-$) and aluminum hydrides (AlH_4^-, $Al_2H_7^-$), highlighting the role of the media in determining their condensed-phase properties and reactivity.

Acknowledgment. This work was supported by the National Science Foundation (CHE01-37627). We thank Profs. John Stanton (University of Texas) and Lee Sunderlin (Northern Illinois Univerisity) for insightful comments and suggestions.

Supporting Information Available: Full citation for ref 37, energy-resolved cross sections for the reaction of AlH_4^- and CH_3O^- with CO_2, competitive modeling fits for the reaction of $Al_2H_7^-$ with CO_2, and fitting parameters. This material is available free of charge via the Internet at http://pubs.acs.org.

JA0424070